Simulation of multilane freeway traffic with detailed rules deduced from microscopic driving behavior

M. Goldbach,* A. Eidmann, and A. Kittel†
Fachbereich Physik, University of Oldenburg, D-26121 Oldenburg, Germany
(Received 7 August 1998; revised manuscript received 28 July 1999)

A simulation to model traffic on a multilane freeway is introduced starting from microscopic driving rules. The model takes each individual car into account with its individual features and actual situations, so that a distribution of parameters as well as different behaviors can easily be analyzed. Therefore, a detailed study of certain situations, driving tactics, vehicle properties, and their influence on the global traffic flow can be performed. The model is discussed, as are first results such as the influence of driver behavior on the fundamental diagram and, in addition, the dynamics of microscopic, individual quantities like separation and difference in speed between successive cars. It turns out that a hysteresis in the reaction of the driver for speeding up and slowing down plays an important role, and effects macroscopic quantities like the shape of the fundamental diagram, e.g., the metastable behavior around the maximum flow and on the speed of observed jams running backward. Furthermore, microscopic time resolved characteristics are strongly influenced, e.g., oscillations in the distance and relative speed between successive cars.

PACS number(s): 05.40.−a, 47.55.−t, 89.40.+k

I. INTRODUCTION

Since our society is more and more dominated by the free flow of goods, and since people are willing to commute longer and longer distances, traffic is a very important and expensive issue in the society of today. The situation becomes even more important if one takes into account the limitation of natural resources like energy and land or the problems originating from pollution. We need models for traffic flow in the future to plan an infrastructure, to control traffic, or even to give politicians and the legislators a base for far reaching decisions. In recent years different attempts have been undertaken to develop fast and reliable algorithms, these attempts ranging from minimal microscopic driving models [1–4], over car-following methods [5,6], to models based on gas kinetics [7–10].

In the present paper we introduce a model of traffic flow which is driven by the idea to be as close as possible to microscopic, i.e., individual, behavior. During the simulation, the state variables of each car, i.e., position, speed, and acceleration, are updated depending on its neighboring cars. The model is, thus, car centered. Nevertheless, the computational efforts are reasonable and the speed of computation is considerably faster than real time even if a standard personal computer is used and 5000 cars are considered. We have chosen highly congested traffic as the initial situation to model the relaxation of a traffic jam. This procedure has the advantage of investigating different values of the density in the traffic flow. As we will see, a variety of different situations with their own characteristics can thus be observed. There is no restriction of the initial situation, and any choice is possible, even a more interesting one: a situation measured from a real traffic situation.

Our first aim is to verify the characteristics of traffic flow as observed in real traffic situations. If the model is able to reproduce these characteristics, it is possible to study the influence of certain parameters, like distribution of a variety of cars (e.g., more or less powerful cars and trucks), different driver behaviors (e.g., more aggressive or passive behaviors), different street features (e.g., number of lanes, inclination), traffic signs (e.g., speed limits, prohibition of passing), driving rules (e.g., to pass on both sides instead of one), and even different weather conditions (e.g., restricted sight due to fog, reduced ability to brake due to slippery streets). All such information can be helpful in the planning of streets, the designing of cars, and the enforcement of laws, as well as in setting up new laws.

In Sec. II we introduce the simulation concept and the microscopic model. Thereafter, in Sec. III, the macroscopic features of the model are discussed and compared to measurements (for clarity, the term ''measurement'' is used throughout the paper to refer to data taken from real traffic, not simulated data). Eventually, some car-following data are presented in Sec. IV, that provide a deeper understanding of the driving behavior.

II. MICROSCOPIC MODEL

The idea of our model originates from the motivation to be as close as possible to the *real* world. The actual state and the individual features of each car, the specific traffic situation, and the behavior of the driver are taken into account during the simulation process. As a consequence, the individual car is represented by a list of variables and parameters characterizing the state and the features, respectively, of each car and driver (simply called ''car'' further on).

In the case of the realization presented in this paper we model three-lane freeway traffic. Each car indexed with i is represented by its actual speed $v^{(i)}$, its actual acceleration $a^{(i)}$, its actual position along the street $x^{(i)}$, and its actual lane $L^{(i)}$ as the state variables with the features, namely,

*Electronic address: goldbach@uni-oldenburg.de
†Electronic address: kittel@uni-oldenburg.de

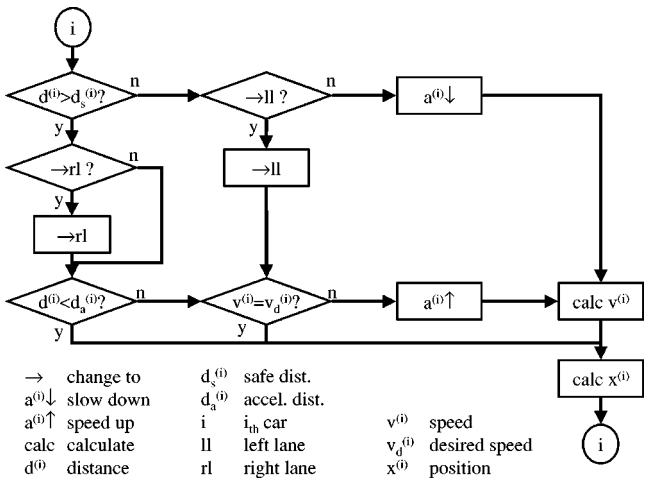

FIG. 1. Flow diagram which is processed for the ith car in one time step. It has to be repeated for all cars during one time step (for details, see text).

desired traveling speed $v_d^{(i)}$, maximum acceleration $a_{max}^{(i)}$, maximum deceleration $a_{min}^{(i)}$, and a factor of no reaction $f_n^{(i)}$, explained in detail below. All cars are organized in a so-called linked list ordered with respect to their position along the street, even if they are driving on different lanes. The street, in the present case, is considered to be homogeneous without any local features, i.e., no local inflow or outflow, a constant number of lanes, no speed limit, unlimited sight, no inclination, and so on. Actually, all these features can be easily incorporated within the model to simulate very special situations and, by means of this, to solve very specific problems. All changes of the cars during one time step ($\Delta t = 0.05$ s) are determined before changing the state of the entire street at once; this is necessary to avoid any artifacts. During all computations floating point operations are used. The model is, thus, continuous. The entire list is updated from the last car to the first one on the street.

At the beginning we initialize the desired traveling speed (DTS) using a Gaussian distribution with a mean value of 33 m/s, a standard deviation of 8 m/s, and a lower cutoff at 22 m/s (80 km/h). All cars have an increasing index i along the direction of driving and have the same length $s^{(i)} \equiv s = 5$ m. They are put on a three-lane street with a period of 10 m. Taking into account the space needed by a car of $s = 5$ m, this period corresponds to a spacing of 25 m for each lane. The initial speed $v^{(i)}$ is set to the minimum of the corresponding DTS $v_d^{(i)}$ and 40 m/s. Their individual speed $v^{(i)}$ is set to the DTS in case it is lower than 40 m/s (144 km/h). The speed of cars with a DTS higher than 40 m/s is set to this value in order to avoid accidents in this highly congested initial situation. In the present paper, the maximum acceleration, the maximum deceleration, and the no-reaction factor are chosen to be equal for all cars, $a_{max}^{(i)} \equiv a_{max} = 1$ m/s^2, $a_{min}^{(i)} \equiv a_{min} = -15$ m/s^2, and $f_n^{(i)} \equiv f_n$, respectively.

Each car is updated in the following way (see Fig. 1). First, the distance $d^{(i)}$ to the car in front is compared to its safe distance $d_s^{(i)}$, i.e., the distance necessary to avoid an accident. The safe distance $d_s^{(i)}$ is defined as

$$d_s^{(i)} = f_s v^{(i)} + s, \tag{1}$$

where f_s denotes a safety factor, which is 1.8 s according to a rule of thumb taught in German driving schools.

If $d^{(i)}$ is smaller than the safe distance $d_s^{(i)}$, the car has to react in the following manner: If there is no possibility to move to the left lane, it has to slow down. We have chosen a detailed braking rule to determine the deceleration (negative $a^{(i)}$) to be sure to avoid accidents. The deceleration is dependent on the distance from the car in front, $d^{(i)}$; the speed of the car in front, $v^{(f)}$; the acceleration of the car in front, $a^{(f)}$; and the speed of the car, $v^{(i)}$. If the distance from the car in front becomes smaller than $d_s^{(i)}$, the car has to brake, i.e., the acceleration $a^{(i)}$ becomes negative. If, in addition, the car in front is braking ($a^{(f)} < 0$), the ith car brakes with $a^{(i)} = a_{min}$. Such a behavior is plausible because the driver intensively brakes if $d^{(i)} < d_s^{(i)}$ and he can see the brake lights of the car in front. If $d^{(i)} < d_s^{(i)}$, but $d^{(i)}$ is still larger than the stopping distance necessary to adjust $v^{(i)}$ to $v^{(f)}$ at a_{min}, $a^{(i)}$ increases linearly with decreasing $d^{(i)}$. At a distance $d^{(i)}$ equal to the stopping distance, the acceleration $a^{(i)}$ is set to a_{min}. This rule guarantees that there are no accidents.

To be able to simulate a natural behavior of a driver, we introduce a no-reaction factor $f_n \geqslant 1$. This denotes the fact that in reality a driver will never change from acceleration to deceleration at a precise separation from another car (cf. Refs. [11–13]). It is more likely that there is an interval of distances where neither acceleration nor deceleration takes place ($a^{(i)} = 0$). This interval is characterized by the factor of no reaction. If the distance $d^{(i)}$ is less than $d_s^{(i)}$, the car decelerates; in the range $d_s^{(i)} < d^{(i)} \leqslant d_a^{(i)}$ it moves at a constant speed without acceleration or deceleration. If $d^{(i)}$ is larger than $d_a^{(i)}$, with

$$d_a^{(i)} = f_n d_s^{(i)}, \tag{2}$$

and the car is driving at a speed $v^{(i)}$ smaller than its DTS, it will accelerate ($a^{(i)} = a_{max}$).

A change to the left lane is possible if the following conditions are fulfilled: first, the distance to the car following after a lane change has to be larger than $d_r^{(i)}$; second, the car ahead after a lane change has to be further apart than $d_f^{(i)} = d_s^{(i)}$; third, if the car is driving on the rightmost lane a car driving on the leftmost lane has to be further back than $d_r^{(i)}$, to avoid an accident after a lane change of both cars to the center lane. The rear distance $d_r^{(i)}$ is defined as

$$d_r^{(i)} = d_0 \exp(-v^{(i)}/v_0) + s. \tag{3}$$

The two constants d_0 and v_0 are set to 90 m and 27 m/s, respectively. This is a phenomenological rule, and only takes the velocity of the ith car into account. It is based on the idea that it is hard for a driver to make an estimate of the speed of the car behind him. Instead the driver relies on the fact that if he is driving at a high speed, the difference in speed ($v^{(r)} - v^{(i)}$) to an even faster driving car r will be smaller and, therefore, the stopping distance needed by the faster following car will be smaller. Using this rule, accidents will arise if the speed difference to the car in rear is greater than 50 m/s, which is very unlikely. We checked if any accidents occured during the simulation, but we never observed one.

Furthermore, to obey the rule to drive on the rightmost possible lane as usual in most European countries, a lane change to the right is checked. To be able to change lanes to the right, it is necessary that the ith car and the cars in front (fth) and at the rear (rth) driving on the neighboring lane are further apart than $d_f^{(i)}$ and $d_r^{(i)}$, respectively.

After the possibility to change lanes has been checked, the actual acceleration, the actual position, and the actual speed are calculated. This procedure is done for all cars driving on the street. Thereafter, the calculated values become the actual ones, and the entire procedure is performed again as the next time step. We have used different time increments to be sure nothing depends on the size of the time step. It is possible to close the street to a loop to keep the average density on the street constant. Instead we utilized transient behavior starting with a high density evolving in time to scan through different densities.

In Sec. III we present results gained from our model under a variation of different quantities. Certain values determined from the fundamental diagram (a q-n diagram, with q the average local flow, and n the average local density), can be seen in connection to quantities which have been used during the simulation. As a result we observe the connection of quantities fed into the microscopic model [e.g., no-reaction factor f_n, and distribution of DTS $P(v_d)$] and the averaged measures (e.g., density and flow at characteristic positions of the fundamental diagram) gained as an output of the simulation.

III. MACROSCOPIC PHENOMENA

Starting from the initial situation given in Sec. II, the average local density for one lane n and the average local velocity $\overline{v}$ are calculated using the model described in Sec. II (also see Table I). n and $\overline{v}$ are defined as $n \equiv N/(\lambda \Delta x)$ and $\overline{v} \equiv 1/N \Sigma_i v^{(i)}$ where N is the number of cars on the street located within each interval of $\Delta x = 0.25$ km, $\lambda = 3$ is the number of lanes, and $v^{(i)}$ is the velocity of cars indexed with i. The average local density develops in time. A typical situation can be observed which was also found for different initial conditions (e.g., for different values of initial average local densities or for different distributions of the DTS). In the following, we discuss the dependence of characteristic macroscopic quantities on the no-reaction factor f_n. It turns out that the f_n significantly influences these quantities (such as the shape of the fundamental diagram, characteristic points of it, or the jam speed).

Figure 2 exhibits the average local density n both in the space (horizontal) and in the time domain (vertical) as a density plot. The values of n are coded in a linear gray scale which ranges from white to black, connected to $n = 0$ and to $n = 66.7$ vehicles/km, respectively. The no-reaction factor was chosen to be $f_n = 1.2$, which turned out to correspond best to characteristic values reported in Ref. [14]. In the lower white triangle, n equals zero. There is no additional car put into the lanes after the initialization, and all cars have left that region. The upper white triangle indicates that no car has actually yet reached the corresponding region. In the upper left of the plot, the initial situation can be seen. The local density is constant in space x at time $t = 0$. After some minutes, structures in the density have formed which can be seen as contrast in the $n(x,t)$ diagram. There is a wide region of jams with a certain inclination. The slope corresponds to a certain speed of jams running backwards. There is mostly congested traffic flow (often called ''synchronized traffic'' in the literature [14,15]). From about $x = 50$ km, the congested traffic flow merges into an almost laminar one with a lower average local density. In this laminar region, still jams occasionally occur. The jams first develop with a positive jam speed, then they decelerate and reach a constant negative value. The value for the jam speed almost equals the one found in the congested region.

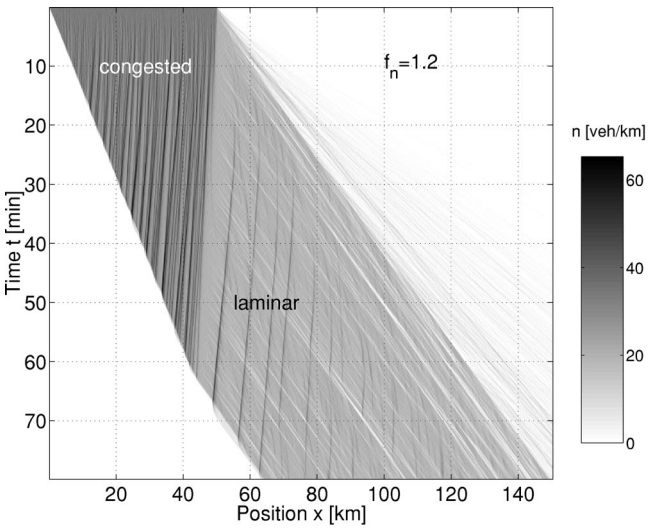

FIG. 2. The average local density n is shown vs space (horizontal) and time (vertical) for a no-reaction factor $f_n = 1.2$ in a density plot. The initial condition is seen in the upper left corner, and $n = 33.3$ vehicles/km is constant in the initial situation. After a transition time, regions of increased local densities occur; in this congested traffic flow, region jams frequently build up. The jams run backwards with a certain velocity. Later on in the plot, laminar traffic flow dominates with some condensations in local density, and occasionally jams occur.

The corresponding fundamental diagram (Fig. 3)—the average local flow $q = n\overline{v}$ depending on density n—is shown as a density plot. For a certain n, we determined the conditional probability density $\mathcal{P}_n(q)$ of the flow q. Its intensity has to be interpreted only in the vertical line (along the fixed n). It is normalized to the corresponding maximum to achieve the best contrast in the plot. Due to the fact that we determine

TABLE I. Simulation parameters.

Acceleration a_s	1 m/s^2
Deceleration a_b	-15 m/s^2
Space needed for one car s	5 m
Safety factor f_s	1.8 s
No-reaction factor f_n	1–2
Desired traveling speed v_d	distributed (see text)
Number of cars	5000
Initial local density	100 vehicles/km
Street configuration	freeway with three lanes
Time step Δt	0.05 s

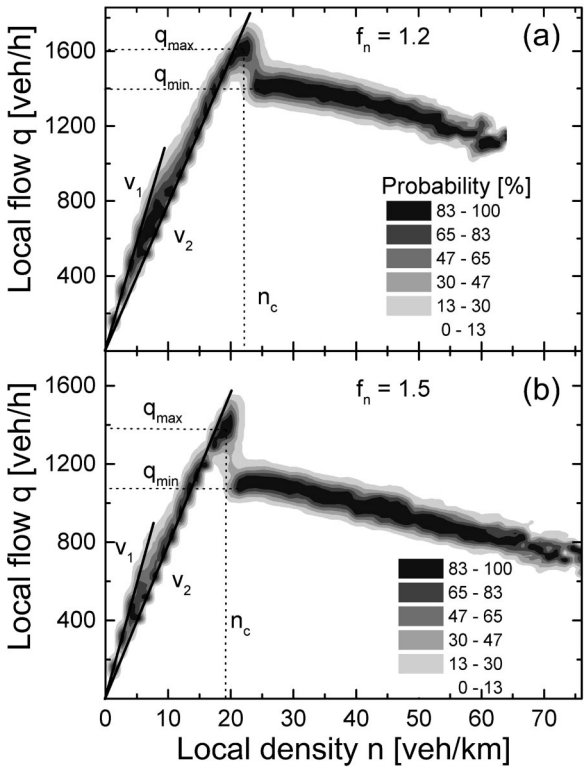

FIG. 3. Fundamental diagram for a three-lane freeway. The probability density $\mathcal{P}_n(q)$ for a given n is plotted vs the average local density n. In plot (a), the no-reaction factor was chosen to $f_n=1.2$, whereas in (b) it is $f_n=1.5$. The probability is normalized to the maximum value of $\mathcal{P}_n(q)$ to reach a maximal contrast. The local density is discrete due to its definition: $n=\text{veh}/\Delta x$ ($\Delta x=0.25$ km). The increasing branch is dominated by the distribution of DTS, whereas the decreasing branch is determined by the accelerating distance $d_a=f_n d_s$. The maximum flow q_{max} and the minimum flow q_{min}, the critical density n_c, and the slopes for free and interacting traffic flow are marked. It is $q_{max}=1620$ vehicles/h, $q_{min}=1400$ vehicles/h, $n_c=23$ vehicles/km, $v_1=33$ m/s, and $v_2=22$ m/s and $q_{max}=1400$ vehicles/h, $q_{min}=1050$ vehicles/h, $n_c=20$ vehicles/km, $v_1=33$m/s, and $v_2=22$ m/s for plots (a) and (b), respectively.

the local density on a certain interval and the integer number of the cars, the local density is discrete with a spacing of $\Delta n=1.33$ vehicles/km, resulting in a wavy structure of the plot. Figure 3(a) was calculated using $f_n=1.2$, and Fig. 3(b) using $f_n=1.5$. First we discuss phenomena which are found for all values of f_n (and are, therefore, equal in both plots). Then we go into details which depend on f_n.

Two branches can be distinguished. The increasing branch shows a slight curvature which can be approximated by two lines with different slopes. We call the first part of the increasing branch *free traffic flow*, and the second one *interacting traffic flow*. The decreasing branch is referred to as *congested traffic flow*. The transition region between both is characterized by *hysteretic traffic flow*. For small local densities $n<8.33$ vehicles/km (i.e., an average distance $d>115$ m between cars on a lane), the flow is determined by the DTS of the individual cars. The slope gives the mean velocity which is about 33 m/s and corresponds to the mean value of the distribution $P(v_d)$ of the DTS. Especially for very low densities, the flow distribution is determined by the one of the DTS. It is

$$\mathcal{P}_{n\to 0}(q)=P\left(\frac{v_d}{\Delta x}\right). \tag{4}$$

For higher densities, $\mathcal{P}_n(q)$ is discussed in the Appendix. We refer to the region of low density as free flow because all cars are moving without any noticeable interaction. For higher average local densities (8.33 vehicles/km $<n<16.67$ vehicles/km) the slope is 22 m/s, and corresponds to the lowest DTS. This means that, for increasing local density, the faster cars are more and more slowed down by the cars with a DTS at the lower end of the distribution (a similar result is reported in Ref. [16]). This region is called interacting traffic flow. Consequently, the distribution density $P(v_d)$ plays only a minor role. In the transition region up to the maximum flow q_{max} at the critical density n_c, the slope (i.e., the mean velocity) further decreases below the lowest value of the DTS [17]. The driving rules for the acceleration and deceleration process begin to determine the traffic flow. The mean spacing of cars is strongly influenced by the mean safe distance $\overline{d_s}$. To study this influence, we introduce an effective no-reaction factor $\tilde{f}_n$ which indicates the dominant driving behavior. The mean spacing $\overline{d}$ of cars can be described by

$$\overline{d}=\tilde{f}_n\overline{d_s}=\tilde{f}_n(f_s\overline{v}+s). \tag{5}$$

If $\tilde{f}_n\approx 1$, all cars move with an almost constant velocity (with a nearly constant separation), and it is $\overline{d}\approx\overline{d_s}$. In contrast, if $\tilde{f}_n\geqslant f_n$, then there is stop-go traffic. Deceleration and acceleration both are important. The cars move with widely distributed velocities which highly fluctuate in time for each car (cf. Sec. IV). Therefore, $\overline{d}$ is increased compared to $\overline{d_s}$. To determine $\tilde{f}_n$ from the flow-density plot, we derive $\tilde{f}_n(q,n)$. It holds that

$$n=\frac{1}{\overline{d}}=\frac{1}{\tilde{f}_n(f_s\overline{v}+s)}, \tag{6}$$

which follows from Eq. (5). Using the definition of the traffic flow $q=n\overline{v}$, the effective no-reaction factor $\tilde{f}_n$ can, thus, be estimated by

$$\tilde{f}_n=\frac{1}{f_s q+sn}. \tag{7}$$

q and n are obtained from the measured data. For $f_n=1.2$, it is $\tilde{f}_n^{max}\approx 1.08$ and $\tilde{f}_n^{min}\approx 1.22$ for $q_{max}\approx 1620$ vehicles/h and $q_{min}\approx 1400$ vehicles/h, respectively, and $n_c=23$ vehicles/km. For $f_n=1.5$, the corresponding values are $\tilde{f}_n^{max}\approx 1.25$ and $\tilde{f}_n^{min}\approx 1.56$ for $q_{max}\approx 1400$ vehicles/h and $q_{min}\approx 1050$ vehicles/h, respectively, and $n_c\approx 20$ vehicles/km.

The difference of the traffic flow in the laminar and congested regions is correlated to the jam speed $\tilde{v}_j$. Such an expression can be formulated as follows: We consider a sec-

tion in the traffic flow around the critical average local density n_c. Using the continuity condition, we can formulate, with $q=n\bar{v}$,

$$q_{max}-q_{min}\equiv n_c(\bar{v}_{max}-\bar{v}_{min})=-n_c v_j . \tag{8}$$

v_j is the jam speed and $v_j\approx -2.57$ m/s as determined from Fig. 3(a). This value is in good agreement with the value of $\tilde{v}_j\approx -2.6$ m/s extracted from the slope of the high density structures in Fig. 2.

The declining branch of the fundamental diagram can be approximated using Eq. (6) by

$$q=\frac{1}{\tilde{f}_n^{min} f_s}-n\frac{s}{f_s} \tag{9}$$

with the empirically determined no-reaction factor $\tilde{f}_n^{min}$. Equation (9) leads to a linear dependence of q on n with a negative slope. The intersection of the extrapolation of the declining branch with the flow axis lies at $q_0=q(n=0)\approx 1670$ vehicles/h in comparison to 1680 vehicles/h obtained from the graphical analysis of Fig. 3(a). The same estimation for $f_n=1.5$ gives $q_0=1290$ vehicles/h compared to 1300 vehicles/h, derived from Fig. 3(b). A slight curvature in the declining part of Fig. 3 can be connected to the fact that the effective no-reaction factor is not constant for increasing n. For $q=0$, it is $n_0\equiv n(q=0)=1/(\tilde{f}_n^{min}s)$. The acceleration of the cars seems to play a less and less important role for increasing densities; therefore, the acceleration rule is less often applied, the effective no-reaction factor $\tilde{f}_n$ decreases and should approach $\tilde{f}_s\approx 1$.

In Fig. 4, q_{max}, $\Delta q=q_{max}-q_{min}$, n_c, and v_j are plotted versus f_n. All values are obtained from the simulations for different no-reaction factors. For $f_n=1$ no jams are found, while for $f_n>1.09$ jams can clearly be observed. All quantities are graphically determined and have an error of about 10%. The maximum traffic flow decreases with increasing f_n. Therefore, the traffic flow is influenced also in the increasing part of the transition region. Such a behavior can be understood from the discussion above. For $f_n<1.1$, it was not possible to identify an abrupt jump in the fundamental diagram. Δq increases with increasing f_n and seems to saturate for higher values. With Eq. (9) it is

$$\Delta q=q_{max}-q_{min}=\frac{1}{f_s}\left(\frac{1}{\tilde{f}_n^{max}}-\frac{1}{\tilde{f}_n^{min}}\right). \tag{10}$$

The difference between the experimentally found values of $\tilde{f}_n^{max}$ and $\tilde{f}_n^{min}$ increases more and more for increasing no-reaction factor f_n. n_c decreases with increasing f_n. A discussion of the quantity has to be done in the frame of a linear stability analysis. The dependence of q_{max} and n_c on f_n are important for an optimal utilization of the street. The jam speed was determined from the density plot. It rises for increasing f_n, shows a maximum for $f_n\approx 1.2$, and decreases afterwards. v_j is connected to Δq with Eq. (8). If we compare the values of q_{max}, Δq, n_c, and v_j to those reported in Ref. [14], we find a good agreement (see Table II) for $f_n\approx 1.2$. The maximum flow is $q_{max}\approx 1600$ vehicles/h, $\Delta q\approx 220$ vehicles/h, $n_c\approx 23$ vehicles/km, and $v_j\approx -10$ km/h. The inflow and outflow are determined by the intersection of the extrapolated declining branch with the increasing one. The mean velocity at this point is given by the lowest DTS, and is 22 m/s in our case.

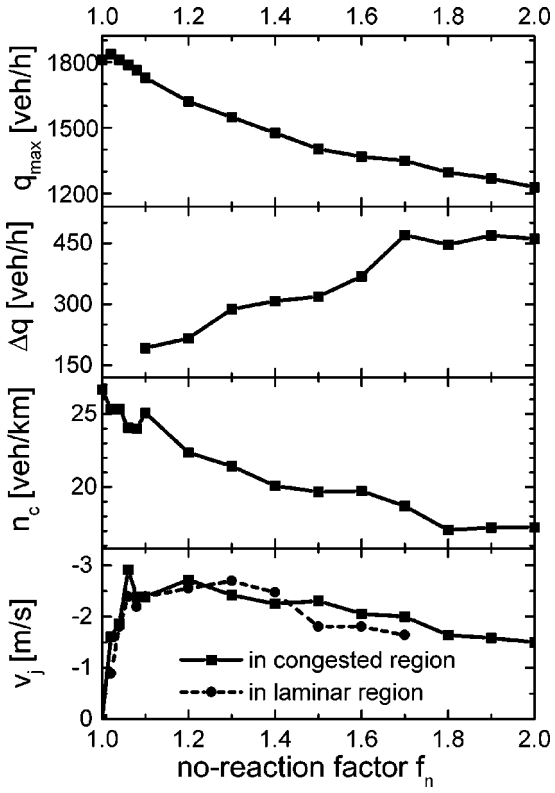

FIG. 4. Dependence of the maximum flow, q_{max}; the difference between the maximum and minimum flows, Δq; the critical density n_c; and the jam speed v_j on the no-reaction factor f_n and displayed.

In this section we discussed the macroscopic phenomena observed in the simulation in detail. We connected them to the driving rules and deduced characteristic quantities such as the jam speed, the inflow and outflow, etc., to the driving behavior of the cars.

IV. MICROSCOPIC PHENOMENA

Next we use car-following methods to look at the individual behavior of a car indexed with p. The time series of the individual speed of a car provides a direct access to the local behavior of the cars, whereas the speed-distance (to the car in front) relation gives the statistical portrayal of the braking and acceleration rules. In a distance to speed difference relation a typical driving scene is caught that gives insight in the driving behavior depending on the car in front.

TABLE II. Comparison: simulation ($f_n=1.2$)—measurement.

	Simulation	Measurement
Jam speed	10 km/h	15 km/h
Inflow/outflow	1400 vehicles/h	1100–1800 vehicles/h
Average speed in the outflow	80 km/h	79–89 km/h
Local density in the outflow	16.7 vehicles/km	17.7 vehicles/km

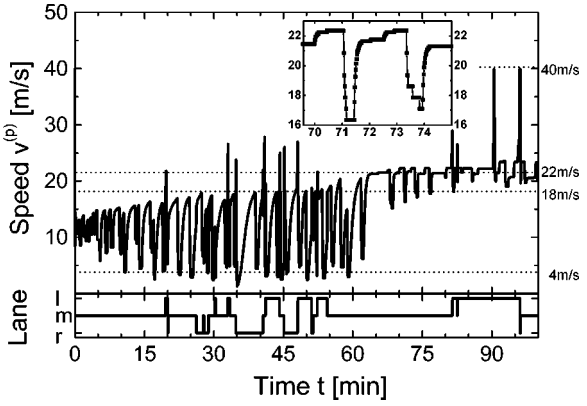

FIG. 5. Time series of the speed for a probe car with the DTS $v_d^{(p)}=40.8$ m/s is plotted vs time for $f_n=1.2$. The probe car moves through jammed regions with stop-go traffic, and those with laminar traffic flow. The inset shows a blow up. Below, the lane used by the probe car is plotted (r, m, and l stand for the right, middle, and left lane).

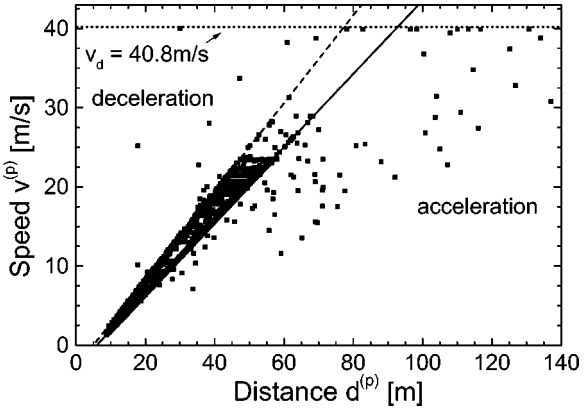

FIG. 6. This diagram portrays the dependence of the speed on the distance to the car ahead for $f_n=1.2$. Therefore, it contains the driving behavior. The dashed line displays the safe distance-velocity relation ($d_s^{(p)}=f_n v^{(p)}+s$), which is the rule for deceleration. The solid line corresponds to the acceleration distance-velocity relation for the acceleration rule ($d_f^{(o)}=f_n d_s^{(p)}$). The dotted line represents the DTS ($v_d^{(p)}$) of the probe car.

Eventually, the probability of the speed with which a car moves is discussed in dependence of the lane it is driving on.

We follow a probe car with a DTS of $v_d^{(p)}=40.8$ m/s. In Fig. 5, a tachogram is shown, whereas the corresponding lane changes are indicated below (r, m, and l referring to the right, middle, and left lane, respectively). Starting from the initial situation where the velocity is set to 40 m/s, the probe car slows down to about 12 m/s. Velocity fluctuations evolve and increase up to $t\approx 15$ min. Their shape remains similar up to $t\approx 65$ min. Such fluctuations range from about 4 to about 18 m/s. At $t\approx 65$ min they decrease dramatically, and the mean velocity of about 22 m/s is found which corresponds to the minimum DTS. Near $t\approx 90$ min, the probe car moves freely for a while and reaches its DTS of $v_d^{(p)}=40.8$ m/s. Such a transient behavior can be understood in the framework of the relaxation of the density. From an initially high density to a finally lower one, the probe car screens different traffic conditions in time, reaching from high congested traffic flow to interacting traffic flow. In the first 65 min the car moves in congested traffic flow. Stop-go traffic can clearly be identified by the large fluctuations in speed and the frequent lane changes. A transition takes place at $t\approx 65$ min (cf. Fig. 2). The inset is a zoom in the time domain (68 min$<t<$75 min), clearly displaying two stop-go events in the laminar traffic flow. The asymmetry between slowing down and speeding up is caused by the difference of the rules for acceleration and deceleration [18].

Now we want to look at the driving behavior, portrayed in Fig. 6 by plotting the speed versus distance of the probe car to the car in front. The region above the horizontal dotted line corresponding to the DTS of the probe car (40.8 m/s) cannot be surmounted, since the rules do not allow to overcome its DTS. The dashed and solid lines correspond to $d^{(p)}=f_n(f_s v^{(p)}+s)$ and $d^{(p)}=f_s v^{(p)}+s$, respectively. In the upper left triangular region above the dashed line, the probe car has to decelerate because its distance to the car ahead is smaller than the safe distance. The region between the dashed and solid lines is the part of no reaction where neither acceleration nor deceleration take place. This region is caused by the existence of the no-reaction factor. Below the solid line, the probe car accelerates to approach its DTS. A very similar plot from a car-following measurement gained from real traffic is shown in Ref. [19]. Since the plot represents congested flow and laminar flow with a mean value of 22 m/s, there is almost no statistical weight at higher velocities.

The difference in speed of the car and the following car, depending on the distance between them, is shown in Fig. 7. It allows a time-resolved analysis of driving behavior. There are oscillations in the distance depending on the speed difference. The amplitudes of these oscillations ($\Delta d\approx 20$ m and $\Delta v\approx 6$ m/s) match with those in Ref. [13]. To distinguish between the two cycles, they are marked with different line types and symbols. The data are taken from the same time interval, as shown in the inset of Fig. 5. The cycles can be divided into six phases. In the first one, the car in front accelerates, and after some time the probe car follows, it accelerates from 21.7 to 22.3 m/s (cf. the first cycle in the inset of Fig. 5), and its distance to the car in front increases to $d^{(p)}=f_n d_s^{(p)}=54$ m. The inset of Fig. 7 shows this behavior in detail. The arrow indicates the direction in time. In phase II

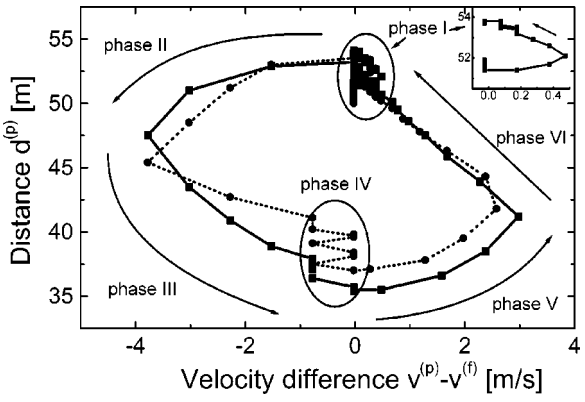

FIG. 7. Dependence of the distance on the difference of speed for $f_n=1.2$. The line is a guide to the eyes. The arrow shows the direction of the time evolution. Six phases can be distinguished, which are discussed in the text.

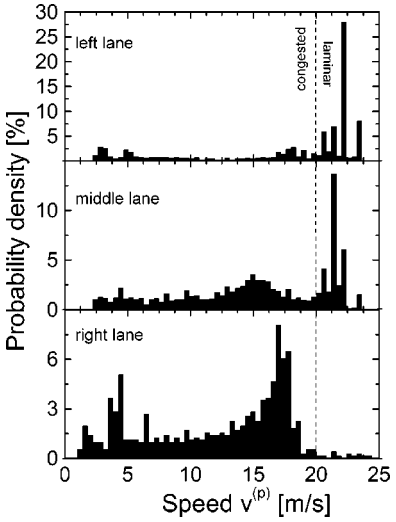

FIG. 8. Probability density of the speed for each lane and $f_n = 1.2$. The lower mean velocities of ≈4 m/s and ≈18 m/s correspond to the lower and upper limits for the velocity fluctuations in the congested traffic flow. The upper mean velocity of ≈22 m/s is the velocity in the laminar flow region. It refers to the lowest velocity of the DTS distribution.

the car in front decelerates but the probe car stays at its velocity until it is $d^{(p)} = d_s^{(p)}$ for the actual velocity of 22.3 m/s. Therefore, the velocity difference becomes negative and the distance between them decreases. In phase III, when the distance is smaller than the safe distance ($d^{(p)} < d_s^{(p)}$), it also decelerates, and the velocity difference vanishes. Its distance is given by $d^{(p)} = d_s^{(p)}$ for the actual velocity of 16.3 m/s (cf. the first cycle of the inset in Fig. 5). In phase IV, the probe car shows an alternating behavior between decelerating and driving at a constant velocity. Such a behavior is more pronounced in the second cycle (also see the inset of Fig. 5, second dip) and originates in the application of the braking rule. In phase V, the car in front accelerates, but the probe car does not follow until its distance from the car in front is increased from $d_s^{(p)}$ to $f_n d_s^{(p)} = 42$ m. At this point both cars accelerate with the same value of 1 m/s^2 starting from different velocities. Therefore, a straight line is found in phase VI.

Phases II and V strongly depend on the no-reaction factor. The variation in distance $\Delta d^{(p)}$ to the car in front in both phases is given by $\Delta d^{(p)} = (f_n - 1) d_s^{(p)}$ and $\Delta d^{(p)} = (1 - f_n) d_s^{(p)}$ for $v^{(p)} = 22.3$ and 16.3 m/s, respectively. Therefore, no oscillations can be found for $f_n = 1$. They arise and increase for higher values of f_n in good agreement with the results obtained from the simulation.

In Fig. 8, the probability density of the velocity $v^{(p)}$ of the probe car is plotted for each lane. There are two regions which refer to the fact that the probe car drives in the congested traffic and in the interacting traffic. First, let us draw attention to the right lane. The probability density is spread out. The distribution exhibits two maxima at about 4 and 18 m/s. These two velocities mark the maximum and minimum velocity fluctuations on average in the congested region. They are labeled in Fig. 5. Such a speed distribution is found in the region of congested traffic flow where stop-go traffic occurs. The probability densities for the middle and left lanes show two contributions. One originates from the driving in congested traffic. Here the probe car is driving with the same distribution in speed on all three lanes; therefore, this phenomenon is called synchronized traffic. The second contribution to the speed distribution stems from the driving in interacting traffic. The first one is equal to that of the right lane, and the second one is quite sharply peaked around 22 m/s. It is labeled in Fig. 5 (see also Ref. [20]). This region corresponds to laminar interacting traffic flow.

V. CONCLUSION

In the present paper we have introduced a model for multilane freeway traffic with rules which are very close to real traffic situations. In the present paper we have restricted our investigations to a specific traffic situation, namely, the relaxation of a highly congested situation on a three-lane freeway. We have discussed in detail the results gained for a distribution of desired speed, detailed rules for braking and lane changes, and a no-reaction factor. The no-reaction factor seems to play an important role. We were able to identify different types of traffic like free traffic flow, interacting traffic flow, the hysteretic transition region, and congested (sometimes called synchronized) traffic flow. We compared macroscopic measures like the maximum flow, the critical density, the jam speed, the inflow and outflow of a jam, the averaged speed in the outflow of a jam, and the local density in the outflow with findings from real traffic. The results in case of a no-reaction factor of 1.2 coincide very well with the experimental data reported in the literature. The influence of the distribution of desired speed and of the no-reaction factor on the observed values of the critical density, the maximum and minimum flow, and the jam speed was discussed in detail. Furthermore, we investigated the microscopic behavior to gain more insight into the individual consequences (like oscillations in the speed difference and distance relative to the car in front, statistics of the speed, and lanes used) depending on the quantities mentioned above. Again, our observations correspond with the measurements reported in the literature.

Due to the car-centered concept, it is possible to incorporate detailed and specific properties of the driving behavior, of the car, and of the street. It is all fully determined. Although the model is very sophisticated, the time needed to run the simulation is still a lot faster than real time. Hence a forecast is possible by using a measured traffic situation as the initial state for the simulation, and a simulation run which is faster than real time. We are convinced that the model is a powerful tool to investigate everyday problems in traffic.

APPENDIX: CONDITIONED PROBABILITY DENSITY

The probability $\mathcal{P}_n(q)$ conditioned to a fixed value of n can be derived from the probability density $Q^{(n)}(v)$ of the velocity v for a given local density n (i.e., for a certain number N of cars in the interval Δx). For the average local flow, it is

$$q = n\overline{v} = \frac{\sum_{i=1}^{N} v^{(i)}}{\Delta x} = \frac{\sum_{i=1}^{N-1} v^{(i)}}{\Delta x} + \frac{v^{(N)}}{\Delta x}. \tag{A1}$$

The probability density for the flow q is, therefore, given by the probability to find one car at $Q^{(N)}(v^{(1)})$, a second one at $Q^{(N)}(v^{(2)})$, etc., and the last one at $Q^{(N)}(\Delta x q - \Sigma_{i=1}^{N-1} v^{(i)})$ and all other possibilities to have a flow q with N cars. This corresponds to a summation over all velocities except the last one, which assures that the exact flow q is reached. The probability density $\mathcal{P}_n(q)$ for the flow q and a certain n is then calculated as

$$\mathcal{P}_n(q) = \int_{v_1} dv_1 \ldots \int_{v_{N-1}} dv_{N-1} \prod_{i=1}^{N-1} Q^{(n)}(v^{(i)}) Q^{(n)} \times \left(\Delta x q - \sum_{i=1}^{N-1} v^{(i)} \right) \tag{A2}$$

for $N \geqslant 2$. For $N = 1$, it is

$$\mathcal{P}_n(\Delta x q) = Q^{(n)}(\Delta x q) \approx P(v_d). \tag{A3}$$

Since Eq. (A2) consists of multiple convolution terms, $Q^{(n)}(v)$ can be evaluated from $\mathcal{P}_n(q)$ via a Fourier transform. Such an analysis is very interesting and will be discussed elsewhere.

[1] M. Cremer and J. Ludwig, Math. Comput. Simulation **28**, 297 (1986).
[2] K. Nagel and M. Schreckenberg, J. Phys. I **2**, 2221 (1992).
[3] O. Biham, A. Middleton, and D. Levine, Phys. Rev. A **46**, 6124 (1992).
[4] T. Nagatani, Phys. Rev. E **48**, 3290 (1995).
[5] A.D. May, *Traffic Flow Fundamentals* (Prentice Hall, Englewood Cliffs, NJ, 1990).
[6] A.D. Mason and A.W. Woods, Phys. Rev. E **55**, 2203 (1997).
[7] M. Lighthill and G. Whitham, Proc. R. Soc. London, Ser. A **229**, 317 (1955).
[8] B. Kerner and P. Konhäuser, Phys. Rev. E **48**, 2335 (1993).
[9] B. Kerner and P. Konhäuser, Phys. Rev. E **50**, 54 (1994).
[10] D. Helbing, Phys. Rev. E **51**, 3164 (1995).
[11] R.M. Michaels and L.W. Cozan, Highw. Res. Rec. **25**, 1 (1962).
[12] E.P. Todosiev and L.C. Barbosa, Traffic Eng. Control **34**, 17 (1963).
[13] R. Wiedemann, Institut für Verkehrswesen, University of Karlsruhe, Heft 8 (1974).
[14] B.S. Kerner and H. Rehborn, Phys. Rev. E **53**, R1297 (1996).
[15] B.S. Kerner, S.L. Klenov, and P. Konhäuser, Phys. Rev. E **56**, 4200 (1997).
[16] E. Ben-Naim and P.L. Krapivsky, Phys. Rev. E **56**, 6680 (1997).
[17] J. Krug and P.A. Ferrari, J. Phys. A **29**, L465 (1996).
[18] S. Krauß, in *Proceedings of Traffic and Granular Flow*, edited by M. Schreckenberg and D.E. Wolf (Springer, Singapore, 1997), p. 271.
[19] Y. Sugiyama, in *Dynamical model for Congestion of Freeway Traffic and its Structural Stability* (World Scientific, Singapore, 1995), p. 137.
[20] D. Helbing, Phys. Rev. E **55**, 3735 (1997).